JACS
JOURNAL OF THE AMERICAN CHEMICAL SOCIETY

pubs.acs.org/JACS

Communication

Pyridine-Conjugated Pillar[5]arene: From Molecular Crystals of Blue Luminescence to Red-Emissive Coordination Nanocrystals

Xin-Yue Lou and Ying-Wei Yang*

Cite This: *J. Am. Chem. Soc.* 2021, 143, 11976−11981

Read Online

ACCESS | Metrics & More | Article Recommendations | Supporting Information

ABSTRACT: A luminescent molecular crystal (P5bipy) and a Cu(I)-coordinated luminescent nanocrystal (Cu(I)-P5bipy) have been prepared concurrently using one conjugated pillar[5]arene macrocycle via a facile supramolecular self-assembling strategy. The molecular crystal shows enhanced luminescence compared with unmodified pillar[5]arene, attributed to its conjugated structure and staggered packing mode, while the coordination nanocrystal exhibits well-defined crystalline structures and long-lifetime triplet state emission along with pronounced solvochromic features.

Supramolecular self-assembly materials elaborated via bottom-up approaches have long been an eye-catching research topic within the realm of chemistry and materials science.[1,2] Among the cohorts of self-assembly systems, supramolecular crystalline materials have attracted considerable interest, especially those with outstanding optical and photoluminescent properties, because of their well-defined architectures and tunable structure−property relationship.[3] Notably, two of the most extensively investigated types of organic luminescent crystals, i.e., organic molecular crystals and metal−organic coordinated crystals, both highly depend on supramolecular self-assembly processes.[4,5] However, the synchronous fabrication of both crystals on the basis of one single molecular entity, which would hopefully enrich the supramolecular approaches for material design, has rarely been reported.

Pillar[*n*]arenes (pillararenes) have been developing rapidly as an attractive and emerging member of supramolecular macrocycles since 2008 and have shown great promise in the fabrication of various materials for divergent applications.[6−12] The rigid pillar architectures of pillararenes allow infinite possibilities in the construction of molecular crystals that can be aimed at applications including vapochromic sensors and gas separation.[5,13−18] Moreover, with versatile potentials of modification on their rims, pillararenes can be effectively equipped with substituents for different functionalities, which significantly assists their further hybridization into metal−organic materials.[19−23] For instance, Stoddart and co-workers reported the crystal growth of a difunctionalized conjugated pillar[5]arene and the incorporation of this pillararene strut into metal−organic frameworks (MOFs).[24] More recently, Huang and co-workers concurrently obtained the molecular crystals and coordinated platinum triangle structures with unique circularly polarized luminescence (CPL) using one conjugated pillar[5]arene molecule.[25] In our previous work, a conjugated pillar[5]arene modified with two pyridine moieties on the *para* positions of one benzene ring, namely, P5bipy (Scheme 1), has been used as a macrocycle ligand to construct a dual-ligand hybrid material with tunable luminescence by coordinating to Cd(II).[26]

Herein, considering the extended π-conjugated structure and the coordination capacity bestowed to P5bipy, we report on the use of P5bipy to fabricate molecular crystals with enhanced blue fluorescence and meanwhile shed light on the luminescent nanocrystals constructed with P5bipy and Cu(I) due to the rich coordination chemistry and photoluminescent properties of Cu(I) iodide clusters (Scheme 1). In this system, a facile supramolecular self-assembly strategy has been demonstrated without sophisticated crystal engineering operations. This also represents the successful fabrication of coordination nanocrystals with intense luminescence and well-defined crystalline structures that adopt synthetic pillararenes as the macrocycle ligands.

P5bipy was synthesized using methoxypillar[5]arene (MeP5) as the starting macrocycle via a multistep modification route as reported previously by us (Figure 1a, Scheme S1, Figures S1−S4).[26] Because of the π-extended structure of P5bipy with two pyridine groups equipped on both rims, one can rationally expect that P5bipy would show optimized photoluminescent properties in its crystal state in comparison with the unmodified MeP5. In this work, both crystals of MeP5 and P5bipy have been obtained and then observed under an optical microscope, where the P5bipy crystal showed an intense mazarine luminescence under 365 nm UV irradiation, whereas MeP5 showed an extremely weak violet emission at the edges of the crystal (Figure 1b). Correspondingly, the photoluminescence quantum efficiency (PLQE) and fluorescence lifetime (τ) of P5bipy crystals were measured to be 1.93% and 13.0 ns, respectively, much higher than that of

Received: July 6, 2021
Published: July 28, 2021

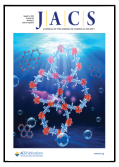

https://doi.org/10.1021/jacs.1c07006

Scheme 1. Chemical Structure of P5bipy, the Formation of Luminescent Molecular Crystals (Single-Crystal Structure) via Crystal Growth, and Coordination-Driven Luminescent Cu(I)-P5bipy Nanocrystals (Simulated Structure)[a]

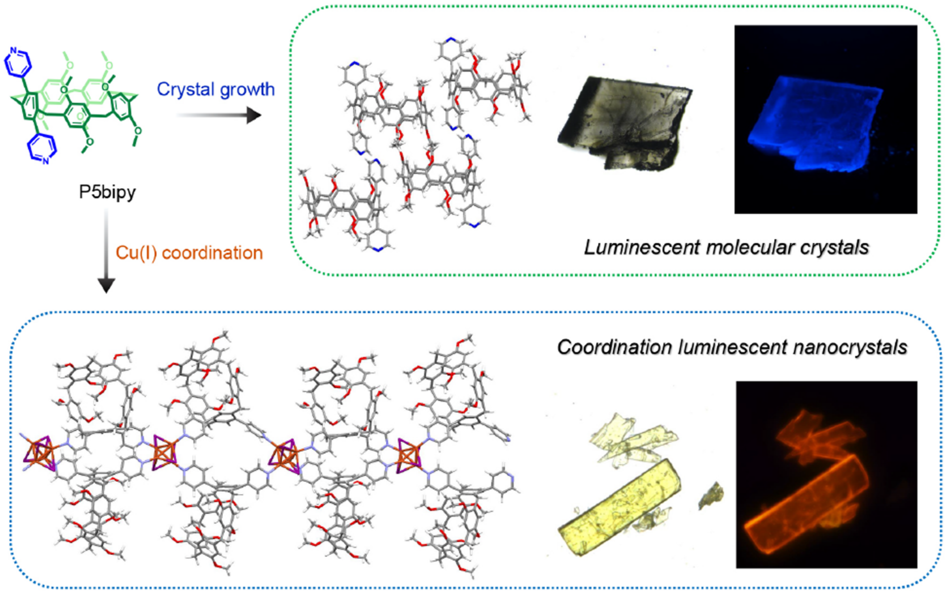

[a]Inset: Microscope images of P5bipy crystals and Cu(I)-P5bipy nanocrystals under sunlight and UV light (365 nm).

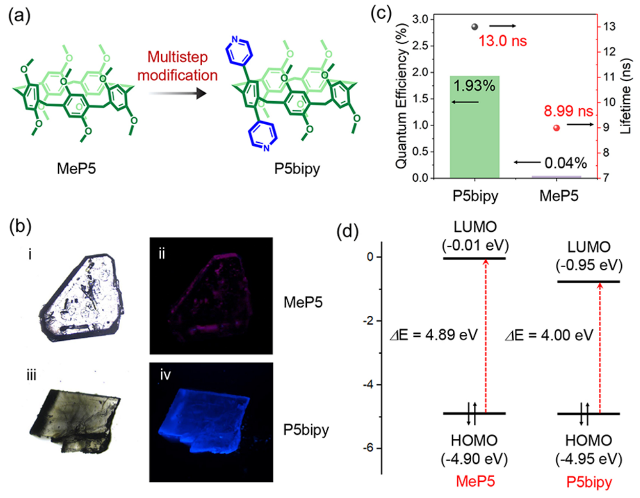

Figure 1. (a) Multistep modification from MeP5 to P5bipy. (b) Optical microscopy images of MeP5 and P5bipy molecular crystals in bright field and under 365 nm UV light in dark field, respectively (10 × 10 times scope). (c) PLQE and luminescent lifetime (τ) of P5bipy and MeP5. (d) Frontier molecular orbitals of MeP5 and P5bipy by DFT calculations.

MeP5 (0.04% and 8.99 ns), indicating the enhanced emission property of P5bipy (Figure 1c and Figure S5). In addition, the energy levels of highest occupied molecular orbital (HOMO) and lowest unoccupied molecular orbital (LUMO) orbitals of MeP5 and P5bipy have been obtained via density functional theory (DFT) calculations (Figure 1d and Figure S6), which also well match their different emission maxima in the crystalline state.

To gain a deeper understanding of the structure−property relationship of P5bipy, the single crystals of P5bipy grown via slow evaporation from a mixed solvent of $CHCl_3$/hexane were examined with single-crystal X-ray analysis (Figure S7 and Table S1). First of all, the presence of enantiomers (*pR* and *pS*) of P5bipy is found in one unit cell in C_2 symmetry (Figure 2a), which is consistent with the literature report.[27] The distance from the functionalized phenyl centroid to the pyridine nitrogen atom is 5.7 Å (Figure S8a), larger than the cavity diameter of pillar[5]arene (ca. 4.7 Å).[6] This size difference gives rise to the restricted inversion of the macrocycle and the fixed planar chirality of P5bipy. The molecular arrangements from the top view and side view are presented (Figure 2b,c), demonstrating a compact packing manner in the (0,0,1) direction perpendicular to the pillar structures and an interlaced zigzag pattern in the (1,0,0) direction along the conjugated axle. No face-to-face stacking is observed among pyridine moieties of adjacent P5bipy molecules, and $\pi-\pi$ interactions between the backbone phenyl rings are absent. Instead, P5bipy molecules in the single-crystal structure are preferably arranged in a staggered manner because of the large dihedral angle (59.71°) between the pyridine groups in *para* positions (Figure 2d). Moreover, the zigzag packing mode can also be stabilized by the intermolecular C−H···O interactions between methoxy groups and methylene bridges of adjacent P5bipy rings (Figures 2d and S8b−d). Intriguingly, layer-by-layer stacking of P5bipy has been observed, where each layer is composed of one enantiomer in uniform chirality, with the *pR* and *pS* forms appearing alternately (Figure 2e), yet showing no chirality on the whole (Figure S9). This mismatching in chirality of each adjoining layer can be regarded as another seminal factor for the unique molecular arrangement of staggered packing fashion. Contributed by the twisted substitution groups and fixed chirality feature, P5bipy is endowed with a distinctive molecular packing mode in the single crystals, which further results in the predictable enhanced luminescent properties.

Next, P5bipy was further used to construct supramolecular coordination complexes with luminescent properties using Cu(I) as the metal nodes, denoted as Cu(I)-P5bipy. Cu(I)-P5bipy was prepared as a yellow granular precipitate by stirring CuI and P5bipy in a molar ratio of 2:1 in CH_3CN/dimethyl

https://doi.org/10.1021/jacs.1c07006
J. Am. Chem. Soc. 2021, 143, 11976−11981

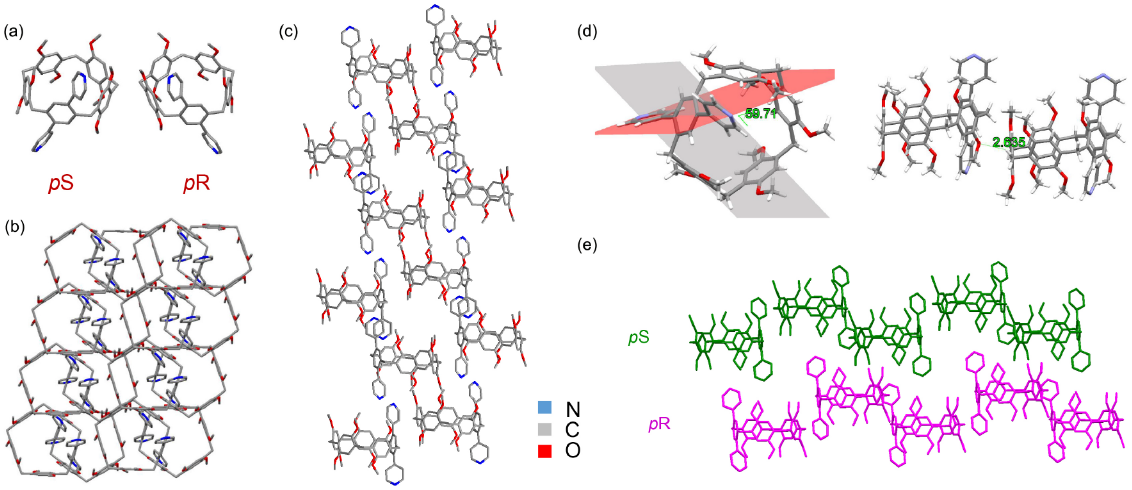

Figure 2. Single-crystal analysis of P5bipy. H atoms in (a), (b), (c), and (e) and solvent molecules are removed from the crystal structure for clarity. (a) *pS* (left) and *pR* (right) enantiomers of P5bipy due to the planar chirality. (b) Staggered packing mode of P5bipy observed along the [001] and (c) [100] directions. (d) Torsion angle between two pyridine groups in the *para* position (left) and C−H···O interaction between adjacent P5bipy molecules (right). (e) Layer-by-layer stacking mode of P5bipy single crystals with alternate enantiomers.

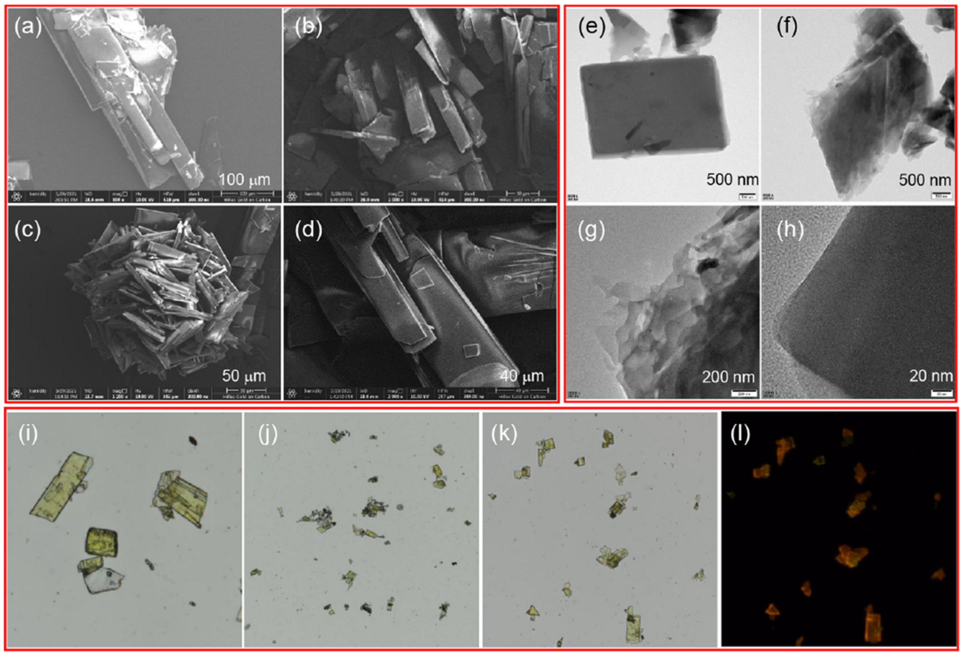

Figure 3. (a−d) SEM images, (e, f) TEM images, and (i−l) optical microscopy images of Cu(I)-P5bipy (i−k: bright field; *l*: 365 nm UV irradiation in dark field; i: 10 × 40 times scope; j−l: 10 × 20 times scope).

sulfoxide (DMSO) (1:1) for 20 min and allowing the mixture to stand for 72 h. The formation of coordinated complexes was fully characterized by various techniques (Figures S10−S14). According to scanning electron microscopy (SEM), transmission electron microscopy (TEM), and optical microscopy, Cu(I)-P5bipy is in the form of transparent nanocrystals with a morphology of block-shaped flakes with thin layers (Figure 3). Although the nanocrystals are unfavorable for single-crystal X-ray analysis, more penetrative information on the crystalline structure of Cu(I)-P5bipy can be given by high-resolution transmission electron microscopy (HR-TEM). As in Figure 4a, clear crystal lattice fringes are observed with the distances of fringes measured to be 0.28 nm, indicating good crystallinity of Cu(I)-P5bipy. The electron diffraction pattern also suggests a polycrystalline structure of Cu(I)-P5bipy nanocrystals by the clear Debye−Scherrer diffraction rings (Figure 4b).

To gain further insight on the coordinated structure, the model of the nanocrystal was simulated using Accelarys Materials Studio 7.0 software based on HR-TEM results and the atomic ratio decided by elemental analysis (Figure S13 and Table S2). The equimolar ratio between Cu and I suggested the metal cluster to be either a dinuclear Cu_2I_2 core or a Cu_4I_4 tetramer, which represent the two most typical structures for Cu(I) in coordination complexes.[28] Universally, unless in overcrowded coordination environments, both clusters adopt four ligands upon formation of metal−organic complexes with a composition of $[Cu_2I_2L_4]$ and $[Cu_4I_4L_4]$, respectively. However, considering the 1:1 relationship of Cu(I) and N of pyridine moieties, the coordination manner of $[Cu_2I_2L_4]$ can

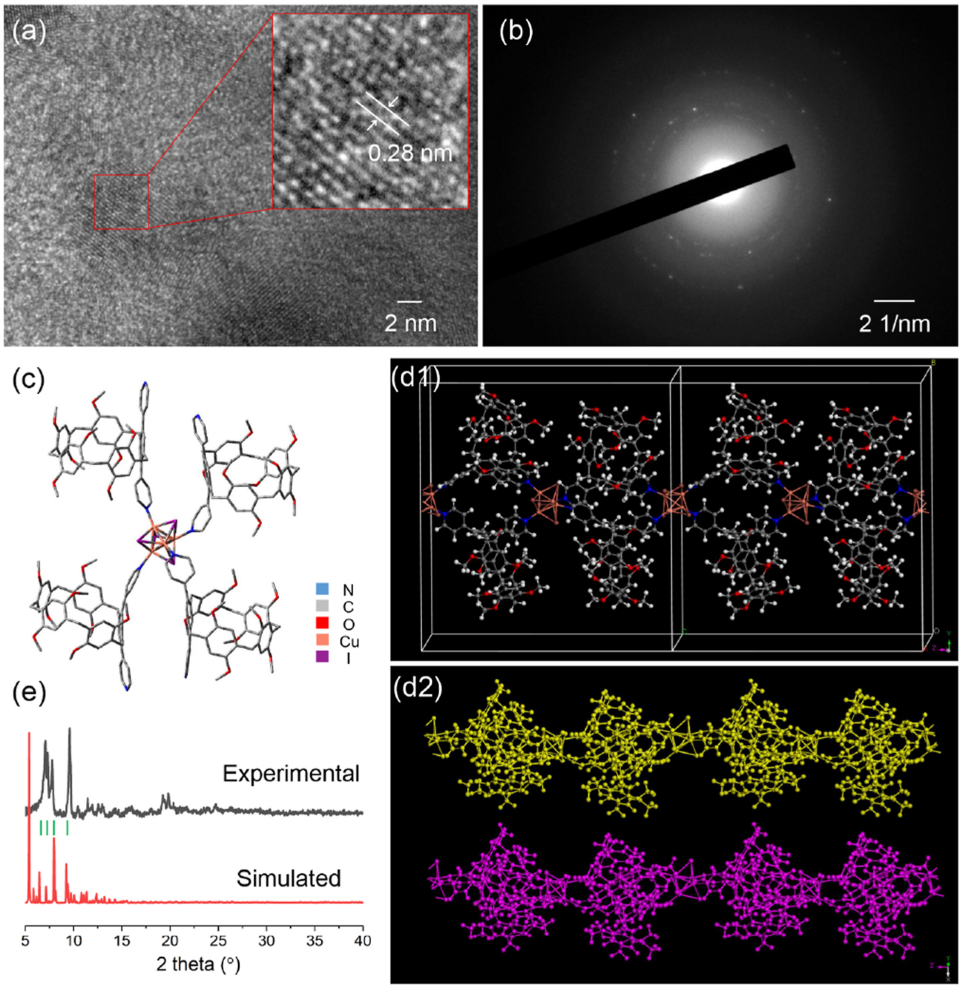

Figure 4. (a) HR-TEM image of Cu(I)-P5bipy. Inset: Magnified image of the marked region. (b) Corresponding electron diffraction pattern. (c) Simulated structure of one structural unit of Cu(I)-P5bipy following the [$Cu_4I_4L_4$] pattern. (d1) Model of the linear supramolecular assembly Cu(I)-P5bipy based on the structural unit in (c); (d2) the stacking between the assemblies (AA manner). (e) Experimental (black) and simulated (red) PXRD patterns of Cu(I)-P5bipy.

be excluded, which would definitely result in a 1:2 ratio between the two atoms. Based on this point, the [$Cu_4I_4L_4$]-type coordination is comparably more possible between the P5bipy macrocycle and Cu(I) cores. Thus, one structural unit of the coordination assembly with a 4:4 pattern was modeled and optimized, composed of a cubane-like Cu_4I_4 coordination core that is attached by four P5bipy bridges (Figure 4c). Notably, the adjacent two P5bipy in the optimized model are in a parallel position with the pyridine groups rather close to each other, which largely favors their mutual coordination to another Cu_4I_4 core. Henceforth, this coordination pattern would lead to a linear assembly, and the rigidity of the assembly can expectedly be guaranteed, since the variance of the pillararene ring orientation is severely restricted due to the parallel arrangement of P5bipy (Figure 4d and Table S3). The simulated powder X-ray diffraction (PXRD) pattern, though not a perfect match, agrees nicely with the experimental data (Figure 4e). This model might not faithfully represent the exact structure of Cu(I)-P5bipy, but can still serve as a proper illustration for the coordinated nanocrystals that answers to the measured parameters within the reach of simulation.

With the structural models developed, we continue to evaluate the photoluminescent properties of Cu(I)-P5bipy. Bright orange-yellow luminescence of Cu(I)-P5bipy nanocrystals can be observed under UV light (Figure 5a and b). Compared with the uncoordinated P5bipy, the emission of Cu(I)-P5bipy nanocrystals exhibits a large red shift, whose emission peak is located at 570 nm (Figure 5c), along with a rather long lifetime (7.08 μs) at room temperature and an enhanced PLQE (24.86%) (Figure S15). Remarkably, the microsecond-scale lifetime can be essentially prolonged under lower temperature and reduced at higher temperature, as measured from 77 to 377 K (Figure 5d and e, Table S4). The long luminescence lifetime and temperature-dependent property of Cu(I)-P5bipy in the solid state are characteristic of phosphorescent emission, which is in good agreement with the reported Cu(I) coordination materials.[29,30]

Solvochromic properties of Cu(I)-P5bipy nanocrystals have also been investigated. Two different emission bands were observed when the nanocrystals were dispersed in ethanol, acetone, and toluene, locating in the wavelength ranges of 400−450 nm and 460−600 nm, respectively, while only one emission band at 450 nm emerged in the dispersion of DMSO (Figure S16a). Thus, the emission color of Cu(I)-P5bipy in the dispersion state varied from yellow to green, and then to blue, depending on the different solvent species, as verified by the 1931 CIE (Commission Internationale de L'Eclairage) chromaticity diagram (Figure S16b). This captivating tunable

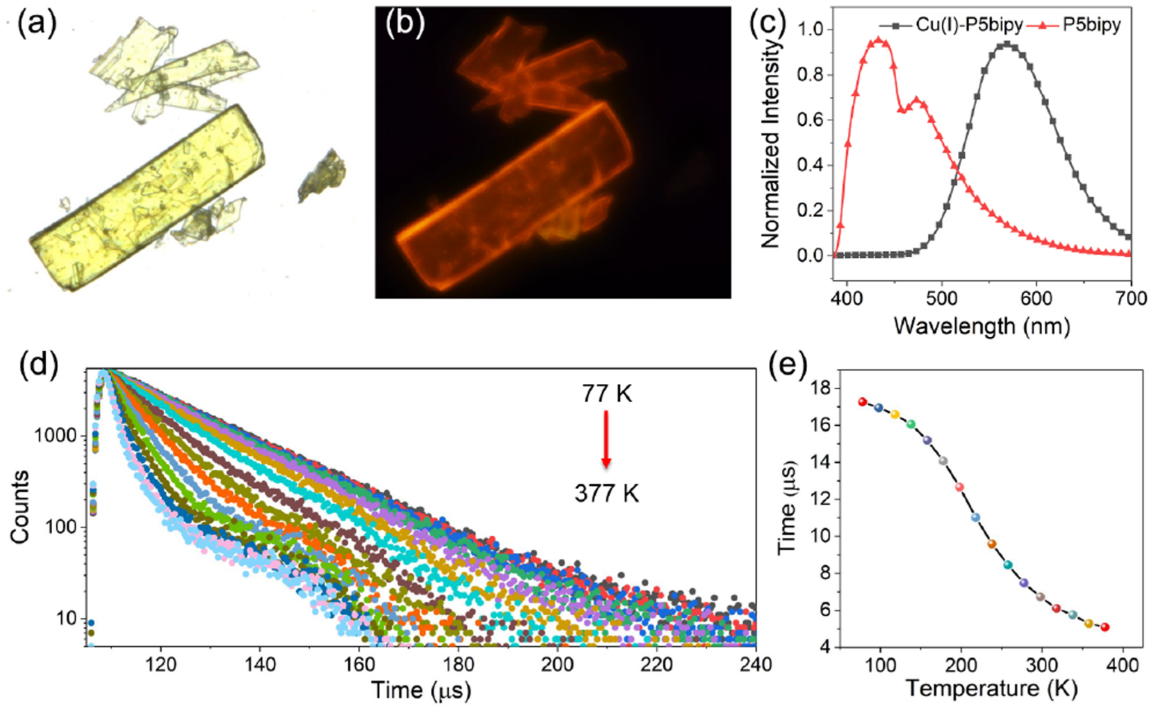

Figure 5. Optical microscopy images of (a) Cu(I)-P5bipy nanocrystal in bright field and (b) under 365 nm UV light in dark field (10 × 40 times scope). (c) Solid-state fluorescence spectra of Cu(I)-P5bipy (black) and P5bipy molecular crystal (red). (d) Emission decay profiles of Cu(I)-P5bipy nanocrystals in the solid state recorded under varied temperature from 77 to 377 K excited at 365 nm. (e) Luminescence lifetime of Cu(I)-P5bipy performed in (d) versus temperature.

emissive feature in different solvent media can be attributed to distinct charge transfer processes within the coordination nanocrystals, whereby the lower energy emission band around 540 nm is due to the halide-to-metal charge transfer (XMCT) of the Cu(I) core, yet the shorter-wavelength emission corresponds to the halide-to-ligand charge transfer (XLCT) and metal-to-ligand charge transfer (MLCT).[28,31−34]

In conclusion, we have concurrently achieved both luminescent molecular crystals and coordination luminescent nanocrystals via facile supramolecular self-assembly processes using a conjugated pillararene, P5bipy. The molecular crystals of P5bipy exhibited enhanced blue luminescence attributed to the π-conjugated dual-pyridine axle and the unique packing fashion in its crystal structure. Furthermore, the nanocrystals with well-ordered crystalline structures and remarkable long-lifetime luminescence were obtained via coordination to Cu(I), which also exhibited tunable emission properties under varied solvent conditions. This work provides a new strategy for developing supramolecular crystal materials with optimized luminescent features, enriching the studies of both supramolecular self-assembly and solid-state light-emitting materials.

■ ASSOCIATED CONTENT

Supporting Information

The Supporting Information is available free of charge at https://pubs.acs.org/doi/10.1021/jacs.1c07006.

> Synthesis and characterization of main compounds and materials; single-crystal analysis; lifetimes and quantum efficiencies, and all experimental details (PDF)

Accession Codes

CCDC 2096367 contains the supplementary crystallographic data for this paper. These data can be obtained free of charge via www.ccdc.cam.ac.uk/data_request/cif, or by emailing data_request@ccdc.cam.ac.uk, or by contacting The Cambridge Crystallographic Data Centre, 12 Union Road, Cambridge CB2 1EZ, UK; fax: +44 1223 336033.

■ AUTHOR INFORMATION

Corresponding Author

Ying-Wei Yang − *International Joint Research Laboratory of Nano-Micro Architecture Chemistry, College of Chemistry, Jilin University, Changchun 130012, People's Republic of China*; orcid.org/0000-0001-8839-8161;
Email: ywyang@jlu.edu.cn

Author

Xin-Yue Lou − *International Joint Research Laboratory of Nano-Micro Architecture Chemistry, College of Chemistry, Jilin University, Changchun 130012, People's Republic of China*

Complete contact information is available at:
https://pubs.acs.org/10.1021/jacs.1c07006

Notes

The authors declare no competing financial interest.

■ ACKNOWLEDGMENTS

The authors acknowledge the National Natural Science Foundation of China (21871108, 51673084) and the Jilin Province University Cooperative Construction Project−Special Funds for New Materials (SXGJSF2017-3) for financial support. This paper is dedicated to the 100th anniversary of Chemistry at Nankai University.

■ REFERENCES

(1) Moulin, E.; Faour, L.; Carmona-Vargas, C. C.; Giuseppone, N. From Molecular Machines to Stimuli-Responsive Materials. *Adv. Mater.* **2020**, *32*, 1906036.

(2) Rest, C.; Kandanelli, R.; Fernandez, G. Strategies to Create Hierarchical Self-Assembled Structures via Cooperative Non-Covalent Interactions. *Chem. Soc. Rev.* **2015**, *44*, 2543−2572.

(3) Maggini, L.; Bonifazi, D. Hierarchised Luminescent Organic Architectures: Design, Synthesis, Self-Assembly, Self-Organisation and Functions. *Chem. Soc. Rev.* **2012**, *41*, 211−241.

(4) Gao, R.; Kodaimati, M. S.; Yan, D. Recent Advances in Persistent Luminescence Based on Molecular Hybrid Materials. *Chem. Soc. Rev.* **2021**, *50*, 5564−5589.

(5) Li, E.; Jie, K.; Liu, M.; Sheng, X.; Zhu, W.; Huang, F. Vapochromic Crystals: Understanding Vapochromism from the Perspective of Crystal Engineering. *Chem. Soc. Rev.* **2020**, *49*, 1517−1544.

(6) Ogoshi, T.; Kanai, S.; Fujinami, S.; Yamagishi, T.; Nakamoto, Y. para-Bridged Symmetrical Pillar[5]arenes: Their Lewis Acid Catalyzed Synthesis and Host-Guest Property. *J. Am. Chem. Soc.* **2008**, *130*, 5022−5023.

(7) Ogoshi, T.; Yamagishi, T.-a. Pillararenes: Versatile Synthetic Receptors for Supramolecular Chemistry. *Eur. J. Org. Chem.* **2013**, *2013*, 2961−2975.

(8) Ogoshi, T.; Yamagishi, T. A.; Nakamoto, Y. Pillar-Shaped Macrocyclic Hosts Pillar[n]arenes: New Key Players for Supramolecular Chemistry. *Chem. Rev.* **2016**, *116*, 7937−8002.

(9) Song, N.; Kakuta, T.; Yamagishi, T.-a.; Yang, Y.-W.; Ogoshi, T. Molecular-Scale Porous Materials Based on Pillar[n]arenes. *Chem.* **2018**, *4*, 2029−2053.

(10) Ogoshi, T.; Kakuta, T.; Yamagishi, T. A. Applications of Pillar[n]arene-Based Supramolecular Assemblies. *Angew. Chem., Int. Ed.* **2019**, *58*, 2197−2206.

(11) Dai, D.; Li, Z.; Yang, J.; Wang, C.; Wu, J.-R.; Wang, Y.; Zhang, D.; Yang, Y.-W. Supramolecular Assembly-Induced Emission Enhancement for Efficient Mercury(II) Detection and Removal. *J. Am. Chem. Soc.* **2019**, *141*, 4756−4763.

(12) Wang, X.-H.; Song, N.; Hou, W.; Wang, C.-Y.; Wang, Y.; Tang, J.; Yang, Y.-W. Efficient Aggregation-Induced Emission Manipulated by Polymer Host Materials. *Adv. Mater.* **2019**, *31*, 1903962.

(13) Li, Q.; Zhu, H.; Huang, F. Alkyl Chain Length-Selective Vapor-Induced Fluorochromism of Pillar[5]arene-Based Nonporous Adaptive Crystals. *J. Am. Chem. Soc.* **2019**, *141*, 13290−13294.

(14) Li, E.; Jie, K.; Fang, Y.; Cai, P.; Huang, F. Transformation of Nonporous Adaptive Pillar[4]arene[1]quinone Crystals into Fluorescent Crystals via Multi-Step Solid-Vapor Postsynthetic Modification for Fluorescence Turn-on Sensing of Ethylenediamine. *J. Am. Chem. Soc.* **2020**, *142*, 15560−15568.

(15) Tan, L.-L.; Li, H.; Tao, Y.; Zhang, S. X.-A.; Wang, B.; Yang, Y.-W. Pillar[5]arene-Based Supramolecular Organic Frameworks for Highly Selective CO_2-Capture at Ambient Conditions. *Adv. Mater.* **2014**, *26*, 7027−7031.

(16) Wu, J.-R.; Yang, Y.-W. Geminiarene: Molecular Scale Dual Selectivity for Chlorobenzene and Chlorocyclohexane Fractionation. *J. Am. Chem. Soc.* **2019**, *141*, 12280−12287.

(17) Wu, J.-R.; Li, B.; Yang, Y.-W. Separation of Bromoalkanes Isomers by Nonporous Adaptive Crystals of Leaning Pillar[6]arene. *Angew. Chem., Int. Ed.* **2020**, *59*, 2251−2255.

(18) Wu, J.-R.; Yang, Y.-W. Synthetic Macrocycle-Based Nonporous Adaptive Crystals for Molecular Separation. *Angew. Chem., Int. Ed.* **2021**, *60*, 1690−1701.

(19) Lou, X.-Y.; Yang, Y.-W. Pillar[n]arene-Based Supramolecular Switches in Solution and on Surfaces. *Adv. Mater.* **2020**, *32*, 2003263.

(20) Li, Z.; Yang, Y.-W. Functional Materials with Pillarene Struts. *Acc. Mater. Res.* **2021**, *2*, 292−305.

(21) Yue, L.; Yang, K.; Lou, X.-Y.; Yang, Y.-W.; Wang, R. Versatile Roles of Macrocycles in Organic-Inorganic Hybrid Materials for Biomedical Applications. *Matter* **2020**, *3*, 1557−1588.

(22) Wang, X.; Liu, Z.-J.; Hill, E. H.; Zheng, Y.; Guo, G.; Wang, Y.; Weiss, P. S.; Yu, J.; Yang, Y.-W. Organic-Inorganic Hybrid Pillarene-Based Nanomaterial for Label-Free Sensing and Catalysis. *Matter* **2019**, *1*, 848−861.

(23) Song, N.; Zhang, Z.; Liu, P.; Dai, D.; Chen, C.; Li, Y.; Wang, L.; Han, T.; Yang, Y.-W.; Wang, D.; Tang, B. Z. Pillar[5]arene-Modified Gold Nanorods as Nanocarriers for Multi-Modal Imaging-Guided Synergistic Photodynamic-Photothermal Therapy. *Adv. Funct. Mater.* **2021**, *31*, 2009924.

(24) Strutt, N. L.; Fairen-Jimenez, D.; Iehl, J.; Lalonde, M. B.; Snurr, R. Q.; Farha, O. K.; Hupp, J. T.; Stoddart, J. F. Incorporation of an A1/A2-Difunctionalized Pillar[5]arene into a Metal-Organic Framework. *J. Am. Chem. Soc.* **2012**, *134*, 17436−17439.

(25) Zhu, H.; Li, Q.; Shi, B.; Xing, H.; Sun, Y.; Lu, S.; Shangguan, L.; Li, X.; Huang, F.; Stang, P. J. Formation of Planar Chiral Platinum Triangles via Pillar[5]arene for Circularly Polarized Luminescence. *J. Am. Chem. Soc.* **2020**, *142*, 17340−17345.

(26) Lou, X.-Y.; Song, N.; Yang, Y.-W. A Stimuli-Responsive Pillar[5]arene-Based Hybrid Material with Enhanced Tunable Multicolor Luminescence and Ion-Sensing Ability. *Natl. Sci. Rev.* **2021**, *8*, No. nwaa281.

(27) Hu, W.-B.; Cai, H.-R.; Hu, W.-J.; Zhao, X.-L.; Liu, Y. A.; Li, J.-S.; Jiang, B.; Wen, K. Pillar[5]arene-Py-Cu Gel, the First Pillar[5]-arene-Based Metallo(organo)gel, and Adsorption of Sudan III by Its Gel-Precipitate. *Eur. J. Inorg. Chem.* **2017**, *2017*, 3551−3554.

(28) Troyano, J.; Zamora, F.; Delgado, S. Copper(I)-Iodide Cluster Structures as Functional and Processable Platform Materials. *Chem. Soc. Rev.* **2021**, *50*, 4606−4628.

(29) Song, Y.; Fan, R.; Wang, P.; Wang, X.; Gao, S.; Du, X.; Yang, Y.; Luan, T. Copper(I)-iodide Based Coordination Polymers: Bifunctional Properties Related to Thermochromism and PMMA-doped Polymer Film Materials. *J. Mater. Chem. C* **2015**, *3*, 6249−6259.

(30) Kobayashi, A.; Fujii, M.; Shigeta, Y.; Yoshida, M.; Kato, M. Quantitative Solvent-Free Thermal Synthesis of Luminescent Cu(I) Coordination Polymers. *Inorg. Chem.* **2019**, *58*, 4456−4464.

(31) Ford, P. C.; Vogler, A. Photochemical and Photophysical Properties of Tetranuclear and Hexanuclear Clusters of Metals with d^{10} and s^2 Electronic Configurations. *Acc. Chem. Res.* **1993**, *26*, 220−226.

(32) Zhou, B.; Xiao, G.; Yan, D. Boosting Wide-Range Tunable Long-Afterglow in 1D Metal-Organic Halide Micro/Nanocrystals for Space/Time-Resolved Information Photonics. *Adv. Mater.* **2021**, *33*, 2007571.

(33) Zhou, B.; Yan, D. Simultaneous Long-Persistent Blue Luminescence and High Quantum Yield within 2D Organic-Metal Halide Perovskite Micro/Nanosheets. *Angew. Chem., Int. Ed.* **2019**, *58*, 15128−15135.

(34) Yan, D.; Evans, D. G. Molecular Crystalline Materials with Tunable Luminescent Properties: From Polymorphs to Multi-Component Solids. *Mater. Horiz.* **2014**, *1*, 46−57.